

# Crystal structure and phase transitions of $\text{Sr}_{1\pm x}\text{Bi}_{2\pm y}\text{Ta}_2\text{O}_9$ ceramics

Jeong Seog Kim <sup>a,\*</sup>, Chae-il Cheon <sup>a</sup>, Hae-Sub Shim <sup>b</sup>, Chang Hee Lee <sup>b</sup>

<sup>a</sup>Department of Materials and Mechanical Engineering, Hoseo University, San 29-1, Sechul-ri, Baebang-myeon, Asan, Chungnam, South Korea, 336-795

<sup>b</sup>Neutron Physics Department, Hanaro Center, KAERI, Daejon, South Korea, 305-600

Received 4 September 2000; received in revised form 6 November 2000; accepted 15 November 2000

## Abstract

Crystal structural parameters, such as space group, lattice parameters, apparent valences (AV), and site occupancies were analyzed in  $\text{Sr}_{1\pm x}\text{Bi}_{2\pm y}\text{Ta}_2\text{O}_9$  ceramics with varying ceramic compositions and diffraction temperature. The crystal structure was refined by Rietveld method using neutron and X-ray powder diffraction data. The phase transition temperature  $T_c$  was measured on these ceramics. The spontaneous polarization  $P_s$  was calculated from the refined parameters. The measured  $T_c$  decreased with increasing Sr-content. The crystal structure of  $\text{Sr}_1\text{Bi}_2\text{Ta}_2\text{O}_9$  changed from A21am at room temperature to B2cb at temperature above 400°C and to a higher symmetry one eventually. The cation place exchanges were observed between  $\text{Sr}^{2+}$  and  $\text{Bi}^{3+}$  and the calculated AVs were in accordance with the cation exchanges. © 2001 Elsevier Science Ltd. All rights reserved.

**Keywords:** Dielectric properties; Phase transition; Tantalates

## 1. Introduction

$\text{SrBi}_2\text{Ta}_2\text{O}_9$  (SBT) is a member of the Bi-layered Aurivillius phase.<sup>1,2</sup> Recently, a great attention has been given to the ferroelectric thin films of SBT due to the potential applications in ferroelectric random access memories.<sup>3</sup> Ferroelectric properties, such as  $P_s$ ,  $E_c$ , and leakage current of SBT thin films have been reported to be critically affected by the chemical composition. The nonstoichiometric compositions with Sr-deficient/Bi-excess have better ferroelectric properties than the stoichiometric.<sup>4,5</sup>

Study on the ferroelectric property-structure relation of the SBT ceramics can provide guidance for a better understanding of the characteristics of SBT thin films. The  $\text{SrBi}_2\text{Ta}_2\text{O}_9$  phase has been reported to have phase transitions at 583 and 843 K related with structural distortions and at room temperature (RT) it becomes a space group A21am.<sup>6</sup> The displacive ferroelectric  $\text{SrBi}_2\text{Ta}_2\text{O}_9$  is described in term of small displacive perturbations away from I4/mmm ( $a'=b'=3.85$  Å) parent structure. However, the crystal structures of the high temperature phases have been remained unresolved due to the experimental and analytical difficulties.

Concerning the crystal structure at RT, some disagreement between the previous reports is found about the cation place exchange. Shimakawa et al.<sup>8</sup> analyzed the structure of the nonstoichiometric  $\text{Sr}_{0.8}\text{Bi}_{2.2}\text{Ta}_2\text{O}_9$  and of stoichiometric  $\text{SrBi}_2\text{Ta}_2\text{O}_9$  using neutron powder diffraction data at RT. The nonstoichiometric composition shows a partial Bi-substitution and cation vacancies at the Sr-site resulting in enhanced ferroelectric polarization. No cation exchange in the stoichiometric composition was found. Contrarily, structural study on the  $\text{ABi}_2\text{Nb}_2\text{O}_9$  (A = Ba, Sr, Ca) shows significant cation placement exchanges between  $\text{A}^{+2}$  and  $\text{Bi}^{+3}$ .<sup>7</sup>

In this study, the crystal structures of high temperature phases were analyzed using high temperature neutron diffraction. The crystal structure and phase transition temperature  $T_c$  with varying Sr-content from Sr-excess to Sr-deficient ceramics were analyzed. For the analysis of cation site occupancies in the structure we used both the X-ray and neutron diffraction data. We found that Rietveld refinement using the X-ray diffraction data led to a false minimum in the oxygen positions, while the neutron diffraction data provided accurate oxygen positions especially in the Bi-layer ceramics due to the smaller scattering power of oxygen compared to the cations. However, in the case of neutron diffraction the scattering powers of Sr- and Bi-ions are very similar to each other, hence the cation site exchange could not be correctly calculated.

\* Corresponding author. Tel.: +82-041-540-5472; fax: +82-041-548-3502.

Therefore, we used a combined refinement method using both X-ray and neutron diffraction data for more accurate analysis on the cation site occupancies. The bond valences were calculated and compared to the refined values of cation place exchanges.

## 2. Experimental

Ceramic samples were prepared by conventional solid-state reaction method. The raw materials,  $Ta_2O_5$ ,  $Bi_2O_3$  and  $SrCO_3$  were mixed in desired proportions by ball-milling. The mixtures were calcined at 900–1100°C for 5 h. The binder-added calcined powder was pressed into discs of 0.5–1 mm thickness and sintered at 1200–1380°C under controlled atmosphere. The permittivities of ceramics were measured at temperatures of 20–600°C using HP4192A impedance analyzer at 100 kHz.

The X-ray powder diffraction data for Rietveld analysis were collected using diffracted beam monochromator,  $CuK\alpha$  rad., 40 kV–40 mA, and 0.02° step scan. Neutron diffraction data were obtained at temperature range of 20–1000°C using HRPD diffractometer at HANARO in KAERI. The neutrons for the Hanaro reactor were monochromatized by a vertically focusing composite Ge-monochromator to a wavelength of 0.18339 nm. The Rietveld refinements were carried out using the program Full-prof.

## 3. Results and discussion

Structural change with ceramic compositions and temperatures were analyzed. Neutron diffraction patterns at RT of the specimens, i.e.  $Sr_{1.2}Bi_{1.8}Ta_2O_9$ ,  $SrBi_2Ta_2O_9$ ,  $Sr_{0.7}Bi_{2.2}Ta_2O_9$  and  $Sr_{0.55}Bi_{2.3}Ta_2O_9$  were judged to be single phase material since no extra reflections could not be found in all of the samples. All of these samples showed reflections. Fig. 1 shows the lattice parameters,  $a$ ,  $b$  and  $c$  with Sr-contents. The polar  $a$ -axis becomes larger

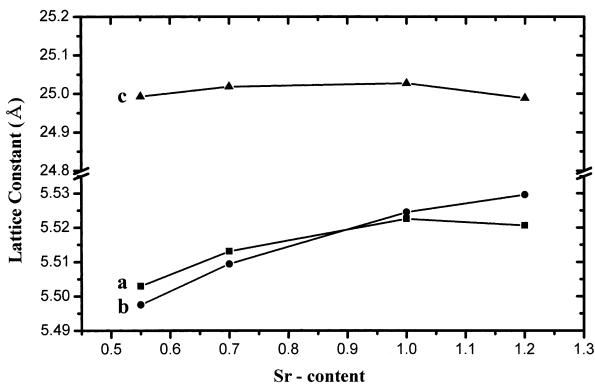


Fig. 1. Lattice parameter change with Sr-contents in the  $Sr_{1\pm x}Bi_{2\pm y}Ta_2O_9$ :  $Sr_{1.2}$  ( $Sr_{1.2}Bi_{1.8}Ta_2O_9$ ),  $Sr_1$  ( $Sr_1Bi_2Ta_2O_9$ ),  $Sr_{0.7}$  ( $Sr_{0.7}Bi_{2.2}Ta_2O_9$ ) and  $Sr_{0.55}$  ( $Sr_{0.55}Bi_{2.3}Ta_2O_9$ ).

than  $b$ -axis with decreasing Sr-content. At room temperature, the crystal structure of space group A21am produced the most reliable  $R$ -values compared to any other possible space groups, such as B2cb, F2mm, I4/mmm, Bbab, and Abam. The refined structural parameters of  $SrBi_2Ta_2O_9$  were identical to the results of Shimakawa et al.<sup>8</sup>

However, the occupational parameters refined by XRD data of  $SrBi_2Ta_2O_9$  in our study showed more than 'full occupancy' that indicated Bi-substitution for Sr-site inconsistently to neutron diffraction analysis. For the precise analysis of the cation site occupancies, a combined refinement method is introduced in which the positional parameters for oxygen ions are refined by the neutron data and the cation occupancies are refined by XRD data. The cation occupations can be more accurately analyzed by using XRD since the scattering amplitudes of the Sr and Bi very differ each other for X-ray but similar in the neutron case. Table 1 shows the refined results of the cation site by the combined method. The Sr-site in  $SrBi_2Ta_2O_9$  shows partial substitution by Bi (0.09). As will be discussed in Fig. 2 the Bi-placement in Sr-site is attributed to the charge imbalance in the Sr-site. The abnormally large thermal parameter of Bi indicates a partial vacancy ( $\approx 0.04$ ) at Bi-site. With the increase of excess-Bi the placement of Bi in the Sr-site increases, and Bi-site is fully occupied by Bi as in the  $Sr_{0.7}$  and  $Sr_{0.55}$  samples shown in Table 1.

In Fig. 2 are shown the calculated apparent valences (AVs) based on bond valence sum rule.<sup>9</sup> The AV of Bi-site is undervalenced and Sr-site is overvalenced. With

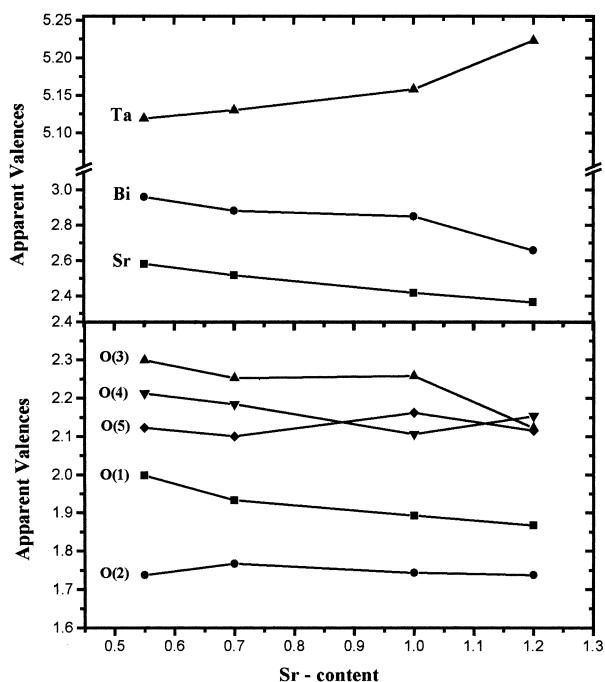


Fig. 2. Calculated apparent valences (AVs) based on the bond valence sum rule using the refined structural parameters.

Table 1

Occupancies of cation sites refined by a combined oxygen positions were refined by using neutron data and cations refined by X-ray diffraction data

Site (atom)	Composition	Sr <sub>1</sub> Bi <sub>2</sub> Ta <sub>2</sub> O <sub>9</sub>		Sr <sub>0.7</sub> Bi <sub>2.2</sub> Ta <sub>2</sub> O <sub>9</sub> <sup>a</sup>		Sr <sub>0.55</sub> Bi <sub>2.3</sub> Ta <sub>2</sub> O <sub>9</sub> <sup>a</sup>	
		Biso (Å <sup>2</sup> )	N (occup.)	Biso (Å <sup>2</sup> )	N (occup.)	Biso (Å <sup>2</sup> )	N (occup.)
Sr	(Sr)	0.50	1.12 (1)	0.50	1.16 (0)	0.50	1.18 (0)
	(Sr/Bi) <sup>b</sup>	0.50	0.90/0.09 (0)	0.50	0.66/0.22 (0)	0.50	0.59/0.27 (0)
Bi	(Bi)	1.80 (0)	1.0	1.16 (1)	1.0	1.25 (0)	1.0
		1.0	0.96 (1) <sup>c</sup>				
Ta	(Ta)	0.15 (0)	1.0	0.17 (0)	1.0	0.31 (0)	1.0
		$R_p = 5.8$	$R_{wp} = 7.79$	$R_p = 5.8$	$R^{wp} = 7.79$	$R_p = 5.8$	$R_{wp} = 7.79$
<i>R</i>		$R_b = 4.01$		$R_b = 4.01$		$R_b = 4.01$	

<sup>a</sup> Refined under a constraint  $2x + 3y = 2$ .<sup>b</sup> Refined by placing both Sr and Bi at Sr-site.<sup>c</sup> Released occupancy by fixing Biso = 1.

increasing Bi-content the AV of Bi-site approaches its formal valence 3 and the Sr-site becomes further overbonded. This enhanced overbonding of Sr-site in the excess-Bi sample is consistent with the place exchange of Sr- and Bi-sites as shown in Table 1. The AV of Ta-site counterbalances the variation of AVs of Bi- and Sr-sites. The AVs of O (1) in Sr-layer and O (3) in Bi-layer apparently decrease with Sr-content in a way to accommodate the decrease of AVs of Bi- and Sr-sites.

Various structural models for the high temperature phases are tested. In Fig. 3 the  $\chi^2 [= (R_{wp}/R_e)^2]$  values are compared for the various structural models with temperatures. Where the  $R_{wp}$  and  $R_e$  are the weighted pattern *R*-factor and the expected *R* factor, respectively, as they are commonly defined in the literatures concerning Rietveld refinement. At room temperature, the A21am model shows incomparably low  $\chi^2$  values to other models. With increasing temperature, the differences in  $\chi^2$  values become reduced and converge to a narrow range (6–8%) at 1000°C. At above 400°C, the B2cb model produced the lowest  $\chi^2$ . Considering that the lattice parameters of the *a*- and *b*-axis are different even at 1000°C, the space group I4/mmm cannot be assigned as the correct model

at 1000°C. Table 2 shows the refined structural parameters using the space group B2cb model.

Fig. 4 shows the dielectric permittivity change with temperature of various Sr-content samples. They show the peaks typical of ferroelectric transitions. The transition peaks shift to high temperature from 290°C in the stoichiometry to 470°C in the Sr-deficient Sr<sub>0.55</sub>Bi<sub>2.3</sub>Ta<sub>2</sub>O<sub>9</sub>. The phase transition peak is completely suppressed in Sr<sub>1.2</sub> sample.

Table 2

Refined structural parameters for at 500°C: space group B2cb,  $a = 5.534(1)$ ,  $b = 5.533(1)$ ,  $c = 25.125(1)$  Å,  $R_p = 7.06\%$ ,  $R_{wp} = 9.40\%$ ,  $R_f = 12.6\%$ ,  $\chi^2[(R_{wp}/R_e)^2] = 7.58$ , N (occupancy) fixed at 1

Atom	<i>x</i>	<i>y</i>	<i>z</i>	Biso (Å <sup>2</sup> )
Sr	0.0	0.0	0.0	1.68 (19)
Bi	0.5158 (43)	0.5099 (25)	0.2008 (2)	1.73 (13)
Ta	0.5114 (51)	0.4977 (2)	10.4156 (2)	0.29 (10)
O1	0.4809 (46)	0.0	0.0	2.23 (30)
O2	0.4608 (54)	0.5250 (36)	0.3410 (3)	1.81 (22)
O3	0.7473 (54)	0.7347 (32)	0.2570 (3)	0.25 (14)
O4	0.2721 (64)	0.7396 (30)	0.0773 (4)	0.68 (21)
O5	0.7488 (66)	1.2276 (34)	0.5742 (6)	2.61 (23)

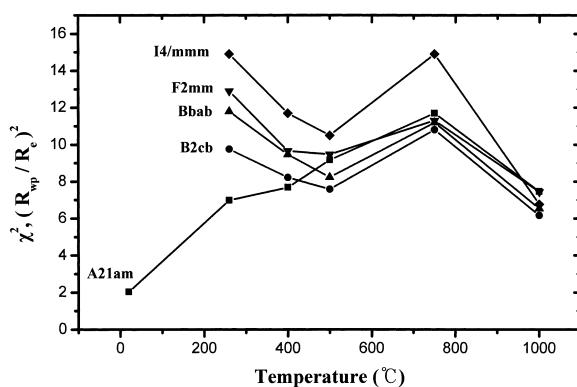
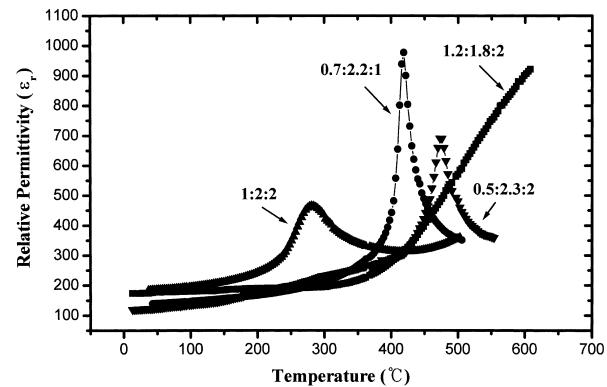
Fig. 3.  $\chi^2 [= (R_{wp}/R_e)^2]$  values of various structural models.

Fig. 4. Dielectric permittivity change with temperature.

In the A21am structure, atomic displacements along the polar axis from the parent structure (I4/mmm) contribute to the spontaneous polarization. The total spontaneous polarization  $P_s$  is calculated as

$$P_s = \sum_j (m_j \cdot \Delta x_j \cdot Q_j e) / v$$

where  $m_j$  is the site multiplicity,  $\Delta x_j$  is the atomic displacement along the  $a$ -axis,  $Q_j e$  is the electric charge of the  $j$ th ions, and  $v$  is the cell volume. The calculated  $P_s$  ( $\mu\text{C}/\text{cm}^2$ ) of the specimens,  $\text{Sr}_{1.2}$ ,  $\text{Sr}_{1.0}$ ,  $\text{Sr}_{0.7}$ , and  $\text{Sr}_{0.55}$ , were 7.1, 15.7, 19.5 and 22.2 respectively. The calculated  $P_s$  increased with Sr-deficiency of the samples. In  $\text{Sr}_{1.2}$  sample the calculated  $P_s$  substantially reduced to  $7.1 \mu\text{C}/\text{cm}^2$ . In the ferroelectric materials large ferroelectric displacement  $\Delta x_j$  is generally related to high  $T_c$  and large  $P_s$ .<sup>10</sup> Therefore, the variation of measured  $T_c$  with ceramic composition agrees with the calculated  $P_s$  change.

#### 4. Conclusion

The crystal structure of  $\text{Sr}_{1\pm x}\text{Bi}_{2\pm y}\text{Ta}_2\text{O}_9$  changes from the orthorhombic A21am to the B2cb at temperature higher than  $400^\circ\text{C}$ . At  $1000^\circ\text{C}$  the  $\chi^2[(R_{\text{wp}}/R_e)^2]$  values for the B2cb, A21am, I4/mmm, F2mm, and Bbab models converge to a narrow range ( $\chi^2=6\text{--}8$ ). This implies that the amplitudes of displacive modulation from the parent I4/mmm become small. The phase transition temperature decreases with the decrease of Bi-content in the sample from  $470^\circ\text{C}$  at  $\text{Sr}_{0.55}\text{Bi}_{2.3}\text{Ta}_2\text{O}_9$  to  $290^\circ\text{C}$  at  $\text{SrBi}_2\text{Ta}_2\text{O}_9$ . The phase transition peak is completely suppressed in  $\text{Sr}_{1.2}\text{Bi}_{1.8}\text{Ta}_2\text{O}_9$  composition. In the stoichiometric  $\text{SrBi}_2\text{Ta}_2\text{O}_9$ , both Bi (0.09) and Sr (0.91) occupy the Sr-site and the placement of Bi ions at Sr-site increased with the excess Bi. The calculated

apparent valences are in agreement with the refined Sr/Bi place exchange values.

#### Acknowledgements

This work was funded by Nuclear Energy Research and Development Supports, MOST, Korea, in the 1999 program year.

#### References

1. Smolenskii, G. A., Isupov, V. A. and Agranovskaya, A. I., Ferroelectric of the oxygen-octahedral type with layered structure. *Soviet Physics-Solid State*, 1961, **3**, 651–655.
2. Aurivillius, B. and Fang, P. H., Ferroelectricity in the compound  $\text{Ba}_2\text{Bi}_4\text{Ti}_5\text{O}_{16}$ . *Phys. Rev.*, 1962, **126**, 893–896.
3. Atsuki, T., Soyama, N., Yonezawa, T. and Ogi, K., Preparation of Bi-based ferroelectric thin films by sol-gel method. *Jpn. J. Appl. Phys.*, 1995, **34**, 5096–5099.
4. Cheon, C. I. and Kim, J. S., Crystal structure, microstructure, and electrical properties in nonstoichiometric SBT thin films. *Integrated Ferroelectrics*, 1998, **21**, 229–240.
5. Watanabe, H., Mihara, T., Yoshimori, H. and Araujo, A. P., Preparation of ferroelectric thin films of Bismuth layer structured compositions. *Jpn. J. Appl.*, 1995, **34**, 5240–5244.
6. Rae, A. D., Thomson, J. G. and Withers, R., Structure refinement of commensurately modulated bismuth strontium tantalate,  $\text{Bi}_2\text{SrTa}_2\text{O}_9$ . *Acta Crystall.*, 1992, **B48**, 418–428.
7. Blake, S. M., Falconer, M. J., McCready, M. and Lightfoot, P., Cation disorder in ferroelectric Aurivillius phases of the type  $\text{Bi}_2\text{ANb}_2\text{O}_9$  ( $\text{A}=\text{Ba}, \text{Sr}, \text{Ca}$ ). *J. Mater. Chem.*, 1997, **7**, 1609–1613.
8. Shimakawa, Y., Kubo, Y., Nakagawa, Y., Kamiyama, T. and Asano, H., Crystal structures and ferroelectric properties of  $\text{SrBi}_2\text{Ta}_2\text{O}_9$  and  $\text{Sr}_{0.8}\text{Bi}_{2.2}\text{Ta}_2\text{O}_9$ . *Appl. Phys. Lett.*, 1999, **74**, 1904–1906.
9. Brown, I. D. and Altermatt, D., Bond-valence parameters obtained from a systematic analysis of the inorganic crystal structure data base. *Acta Crystall.*, 1985, **B41**, 244–247.
10. Abrahams, S. C., Revez, J., Simon, A. and Chaminade, J. P., Ferroelectric behavior and phase transition at 715K in  $\text{SrAlF}_5$ . *J. Appl. Phys.*, 1981, **52**, 4740–4742.